

Influence of crystal-potential fluctuations on Raman spectra of coupled plasmon–LO-phonon modes in disordered systems

Yu. A. Pusep, M. T. O. Silva, and J. C. Galzerani

Universidade Federal de São Carlos, 13565-905 São Carlos, São Paulo, Brazil

N. T. Moshegov

*Instituto de Física de São Carlos, Universidade de São Paulo, 13560-970 São Carlos, São Paulo, Brazil
and Institute of Semiconductor Physics, 630090 Novosibirsk, Russia*

P. Basmaji

*Instituto de Física de São Carlos, Universidade de São Paulo, 13560-970 São Carlos, São Paulo, Brazil
(Received 20 April 1998)*

The effect of the structural disorder in the Raman scattering of the coupled plasmon–LO phonon modes was studied in doped $\text{Al}_x\text{Ga}_{1-x}\text{As}$ alloys and in doped GaAs/AlAs superlattices. It was observed that the asymmetry in the Raman lines, caused by this effect, is opposite to that observed for the optical phonons. This fact is explained by the differences in the dispersion curves of the optical phonons and plasmons—a negative dispersion for the phonons and a positive one for the plasmons. The analysis of the Raman line shapes by means of a Gaussian spatial correlation function allowed us to obtain the localization lengths for the LO phonons and for the plasmons in the alloys and in the superlattices; the dispersions of the coupled plasmon–LO-phonon modes were studied and an evidence for a metal-dielectric transition occurring in superlattices when the lowest miniband is completely occupied was found. [S0163-1829(98)08239-3]

I. INTRODUCTION

Fluctuations of the crystal potential destroy its translational invariance and, as a consequence, a breakdown of the Raman selection rules occurs, leading to the broadening and asymmetry of the Raman lines. This effect was found to determine the shapes of the optical-phonon Raman lines in microcrystalline semiconductor materials¹ and in semiconductor alloys;² moreover, the violation of the coherency of the elementary collective excitations (phonons or plasmons) leads to localization effects. However, to our knowledge, an analysis of the influence of the crystal potential fluctuations on the plasmon Raman lines has not yet been done.

The volume where the collective excitations are localized is determined by a spatial localization length (L); this length can serve as a parameter characterizing the microscopic nature of the crystal potential fluctuations. Then a study of phonons in disordered materials will give us a possibility to characterize the structural quality, while plasmons, in addition, will provide us with information about the influence of the crystal potential fluctuations on the electron transport.

In this paper we study the effect of the crystal-potential fluctuations on the plasmon–LO-phonon Raman scattering in doped $\text{Al}_x\text{Ga}_{1-x}\text{As}$ alloys and in doped $(\text{GaAs})_n(\text{AlAs})_m$ superlattices (n and m are the thicknesses of the corresponding layers expressed in monolayers). Both the systems under consideration reveal fluctuations of the crystal potential caused either by the random alloy potential or by the disordered character of the interface between the GaAs and AlAs layers in superlattices. Moreover, the fluctuations of the impurity potential contribute to both systems as well.

The samples were grown by molecular-beam epitaxy, and

were doped with Si in order to obtain free electron concentrations in the range $(1-5) \times 10^{18} \text{ cm}^{-3}$. $\text{Al}_{0.2}\text{Ga}_{0.8}\text{As}$ alloys $1 \mu\text{m}$ thick were deposited on (100)-oriented GaAs substrates. $(\text{GaAs})_{17}(\text{AlAs})_2$ superlattices (with 20 periods) were also grown on (100) GaAs substrates. The superlattices were prepared with ultrathin AlAs barriers (2 ML thick) in order to allow the occurrence of vertical motion of electrons through the superlattices and, therefore, to study the superlattice plasmons (the plasmons polarized normal to the layers). Backscattering unpolarized Raman spectra were performed at $T=8 \text{ K}$ with a Jobin-Yvon double-grating spectrometer supplied with an usual phot counting system; the 5145-Å line of an Ar^+ laser was utilized for excitation.

II. THEORY

As is well known, in doped semiconductors free electrons electrically couple with the LO phonons, producing coupled plasmon–LO-phonon modes. In the $\text{Al}_x\text{Ga}_{1-x}\text{As}$ alloy and in $(\text{GaAs})_n(\text{AlAs})_m$ superlattices, two types of LO phonons are distinguished: GaAs-like and AlAs-like. The interaction of these phonons with free electrons produces two coupled optical modes ω_1^+ and ω_2^+ ; the first one is due to the coupling of the GaAs-like LO phonons with electrons, while the second one originates from the AlAs-like LO phonons. In addition, the low-frequency acousticlike ω^- coupled mode appears in the frequency range below the frequency of the GaAs-like TO phonon.

Both the deformation potential (DP) and the Fröhlich interaction (FI) mechanisms are responsible for the Raman scattering by the coupled plasmon–LO-phonon modes. In

this case the scattering efficiency close to the E_1 resonance is given by³

$$\frac{\partial^2 R}{\partial \Omega \partial \omega} \sim - \int d^3 q g_r(\mathbf{q}) \cdot f_{sc}(\mathbf{q}) \text{Im} \frac{1}{\epsilon(q, \omega)}, \quad (1)$$

where $g_r(\mathbf{q})$ is the function which takes into consideration the enhancement of the Raman efficiency when the excitation laser has an energy close to the E_1 critical point (this function is different for *DP* and *FL*), $f_{sc}(\mathbf{q}) = [4\pi/(q^2 + q_0^2)]^2$ is the screening correlation function (here q_0 is the screening wave vector), and $\epsilon(q, \omega)$ is the dielectric function which includes contributions due to both optical phonons and plasmons.

According to Ref. 1, the relaxation of the conservation of the crystal momentum caused by the crystal potential fluctuations can be taken into account by introducing a Gaussian spatial correlation function $\exp(-4R^2/L^2)$, which yields

$$\frac{\partial^2 R}{\partial \Omega \partial \omega} \sim - \int d^3 q g_r(\mathbf{q}) \cdot f_{sc}(\mathbf{q}) \exp\left(-\frac{q^2 L^2}{4}\right) \cdot \text{Im} \frac{1}{\epsilon(q, \omega)}. \quad (2)$$

Without loss of generality, far from resonance, the Raman intensity can be written in a phenomenological form

$$I(\omega) \sim \int f_{sc}(\mathbf{q}) \exp\left(-\frac{q^2 L^2}{4}\right) \frac{d^3 q}{[\omega - \omega(q)]^2 + (\Gamma/2)^2}, \quad (3)$$

where $\omega(q)$ is the dispersion of the relevant collective excitations, and Γ is their damping constant.

We used the dispersions of the optical LO phonons for bulk $\text{Al}_x\text{Ga}_{1-x}\text{As}$ in the form

$$\omega(q) = \omega_{\text{LO}}(1 - Aq^2), \quad (4)$$

where ω_{LO} is the frequency of the longitudinal-optical phonons. This formula gives a good approximation of the experimental data⁴ with $A(\text{GaAs}) = 0.18(a/2\pi)^2$ and $A(\text{AlAs}) = 0.05(a/2\pi)^2$, where a is the lattice constant.

The dispersion of the plasmons was taken in the random-phase approximation⁵

$$\omega(q) = \omega_p \left[1 + \frac{3}{10} \left(\frac{v_F}{\omega_p} \right)^2 q^2 \right], \quad (5)$$

where $\omega_p = (4\pi e^2 n/m)^{1/2}$ is the plasma frequency, and v_F is the Fermi velocity.

At the electron densities relevant to the samples under investigation, $\omega_p \approx \omega_{\text{LO}}$; then, the dispersion of the coupled plasmon-LO-phonon modes is almost completely determined by the dispersion of plasmons, which is much stronger than that of the LO phonons.

As it is seen from Eq. (3), the dispersion of collective excitations $\omega(q)$ and the value of the localization length L are responsible for an asymmetry of the Raman line. It follows from Eqs. (3)–(5) that the asymmetry of the plasmon-LO-phonon Raman line should be opposite to that of the LO phonon; this is explained by the different dispersions of the optical phonons and plasmons—a negative dispersion for the LO phonons and a positive one for the plasmons.

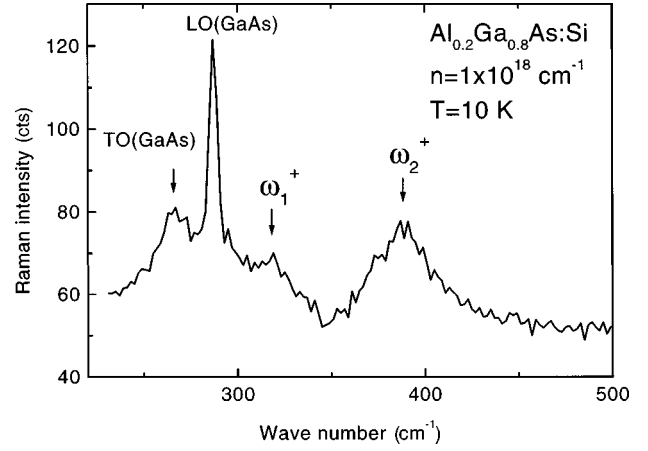


FIG. 1. The Raman spectrum of the doped $\text{Al}_{0.2}\text{Ga}_{0.8}\text{As}$ alloy with an electron density $n = 1 \times 10^{18} \text{ cm}^{-3}$ measured at $T = 8 \text{ K}$.

We assumed an isotropic spatial correlation and a spherical Brillouin zone in alloys. Superlattices present anisotropic systems with the electron energy defined as

$$E(q_{\parallel}, q_z) = \frac{\hbar^2 q_{\parallel}^2}{2m_{\parallel}} + E(q_z), \quad (6)$$

where q_{\parallel} and q_z are the electron momenta parallel and perpendicular to the layers, respectively.

In such anisotropic systems there is no way to take into account the screening effects correctly. Therefore, in superlattices we used the isotropic approximation (3) where all the parameters have a meaning of values averaged over directions. Thus the average dispersion of plasmons was calculated according to Eq. (5) with the average effective mass $\bar{m}^{-1} = \frac{1}{3}(2m_{\parallel}^{-1} + m_z^{-1})$, where the electron effective mass in-plane of the layers m_{\parallel} was taken to be equal to the effective mass of electrons in bulk GaAs ($m = 0.068m_0$), while the effective mass normal to the layers m_z was calculated by the envelope function approximation as has been done in Ref. 6.

In the case of thick enough barriers when quantum wells are well isolated, the only contribution to the Raman intensity is due to the plasmons polarized in plane of the layers (which become active in the backscattering configuration due to the electron scattering); therefore, the problem becomes a two-dimensional one and can be easily solved with an appropriate modification of Eq. (3) and with the two-dimensional screening correlation function⁷ $f_{sc}(\mathbf{q}) = [1/(q + q_0)]$, with $q_0 = 2g_v/a^*$ where g_v is a valley degeneracy factor which gives the number of equivalent energy bands, and a^* is the effective Bohr radius.

III. EXPERIMENTAL RESULTS AND DISCUSSION

The Raman spectra of one of the doped $\text{Al}_{0.2}\text{Ga}_{0.8}\text{As}$ alloys is shown in Fig. 1. The two lines assigned as ω_1^+ and ω_2^+ are the GaAs and AlAs-like coupled modes, respectively. In addition, the TO and LO GaAs-like phonons of the alloy were observed at 266 and 286 cm^{-1} , respectively. The uncoupled LO phonon is seen because of the surface depletion layer.

The Raman spectra measured in the spectral range of the

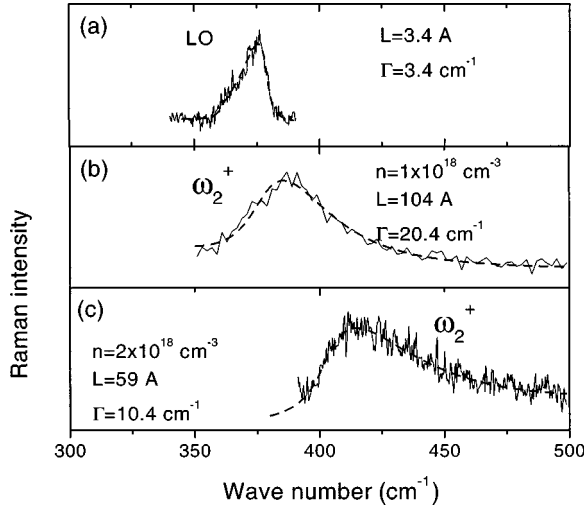


FIG. 2. The Raman spectra of doped $\text{Al}_{0.2}\text{Ga}_{0.8}\text{As}$ alloys with different electron densities measured at $T = 8$ K in the spectral range of AlAs-like optical phonons: intrinsic alloy (a), $n = 1 \times 10^{18} \text{ cm}^{-3}$ (b), and $n = 2 \times 10^{18} \text{ cm}^{-3}$ (c).

AlAs-like LO phonon in the samples with different electron densities are presented in Fig. 2. The asymmetry of the LO Raman line observed in the intrinsic alloy [Fig. 2(a)] was found similar to that observed in $\text{Al}_x\text{Ga}_{1-x}\text{As}$ alloys.² The coupling of the LO phonons with the plasmons in the doped alloy causes a blueshift of the Raman line, and, in addition, drastically changes its shape—the asymmetry of the Raman line becomes opposite to that due to the LO phonons.

As mentioned above, different asymmetries of the LO-phonon line and of the coupled mode line are caused by the different dispersions of the LO phonons and plasmons. The Raman spectra calculated by Eq. (3) with Eqs. (4) and (5) reveal a good fitting to the experimental results with the values of the localization lengths L depicted in Fig. 2. In order to calculate the screening correlation function in the doped alloy, we used the Thomas-Fermi screening radius as the value of q_0 .

If the localization length L is small enough, then collective excitations in a broad interval of their dispersions will be involved in the Raman scattering. In this case the width of the asymmetrical Raman line is determined by the dispersion of the relevant collective excitations. Our results show that the phonon states from almost the whole Brillouin zone contribute to the Raman scattering in the intrinsic $\text{Al}_{0.2}\text{Ga}_{0.8}\text{As}$ alloy because the half-width of the asymmetrical LO-phonon line ($\approx 14 \text{ cm}^{-1}$) is almost equal to the dispersion of the AlAs-like LO phonon ($\approx 20 \text{ cm}^{-1}$).

The situation is somewhat different in the doped alloy where, as is well known, the dispersion of the plasmons is well defined until a critical value of the wave number q_c , while the plasmons with $q > q_c$ decay into single-particle electron excitations.⁵ In the samples studied, the estimates give $q_c \approx 3 \times 10^6$ and $3.6 \times 10^6 \text{ cm}^{-1}$ in the alloys with the electron concentrations $n = 1 \times 10^{18}$ and $2 \times 10^{18} \text{ cm}^{-3}$, respectively; this yields total dispersions of the plasmons of ≈ 46 and $\approx 75 \text{ cm}^{-1}$ in the corresponding samples, while the half-widths of the asymmetrical plasmon-LO-phonon lines are about 40 and 50 cm^{-1} , respectively. This means that the

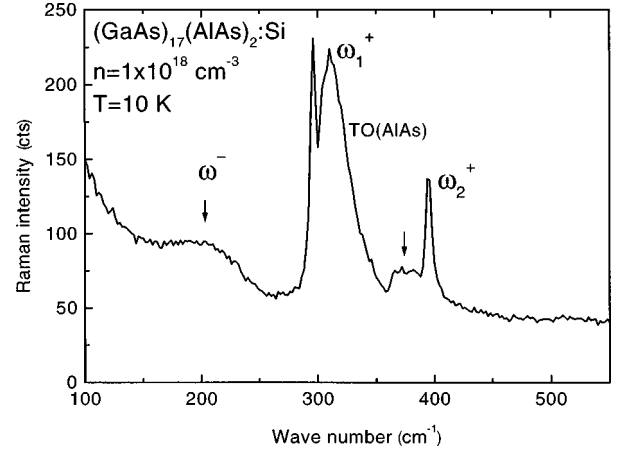


FIG. 3. The Raman spectrum of the doped $(\text{GaAs})_{17}(\text{AlAs})_2$ superlattice with an electron density $n = 1 \times 10^{18} \text{ cm}^{-3}$ measured at $T = 8$ K.

largest part of the available plasmon states contribute to the Raman scattering.

Results similar to those obtained in the doped $\text{Al}_{0.2}\text{Ga}_{0.8}\text{As}$ alloys were observed in the doped $(\text{GaAs})_{17}(\text{AlAs})_2$ superlattices, where Raman lines corresponding to the coupled plasmon-LO-phonon modes revealed the same kind of asymmetry caused by the dispersion of the plasmons. Figure 3 displays the Raman spectrum of a doped $(\text{GaAs})_{17}(\text{AlAs})_2$ superlattice with the electron concentration $n = 1 \times 10^{18} \text{ cm}^{-3}$. Again, as in the alloys, the two coupled modes (GaAs and AlAs-like) were observed, both revealing an inverted asymmetry as compared to the one found for the optical phonon line. Additionally, due to a better structural quality of the superlattices in comparison with the alloys, the low-frequency ω^- coupled mode was observed as well. The LO-phonon line of the GaAs layers was found as a sharp line at 296 cm^{-1} ; as in the case of the doped alloys, it appears to be due to the surface depletion layer. The TO phonon of the AlAs barriers (and probably the LO phonon as well, appearing by the same reason as the LO phonon of the GaAs layers) was found around 370 cm^{-1} . The Raman spectra measured in superlattices with different electron densities are shown in Fig. 4. The spectrum in Fig. 4(a) corresponds to the sample with a partially occupied lowest Γ miniband, while those in Figs. 4(b) and 4(c) were measured in the samples with completely filled lowest Γ minibands, when the Fermi level is located close to the top of the miniband or even in a minigap (see calculations presented for similar samples in Ref. 6). The strong decrease of the localization length L , found when the Fermi level enters a minigap, reflects the localization of electrons and serves as evidence of the metal-dielectric transition which takes place with an increase of the electron density in superlattices. Two effects can be responsible for this localization: the formation of one-dimensional conducting channels in superlattices due to the fluctuations of the electron potential,⁶ and the “reentrant localization” found to occur for the electron states at the top of a miniband.⁸

The percentage of states of the total plasmon dispersion involved in the Raman scattering of the doped superlattices can be estimated from the following data: in the superlattices with the electron concentrations 1×10^{18} , 3×10^{18} , and 5.6

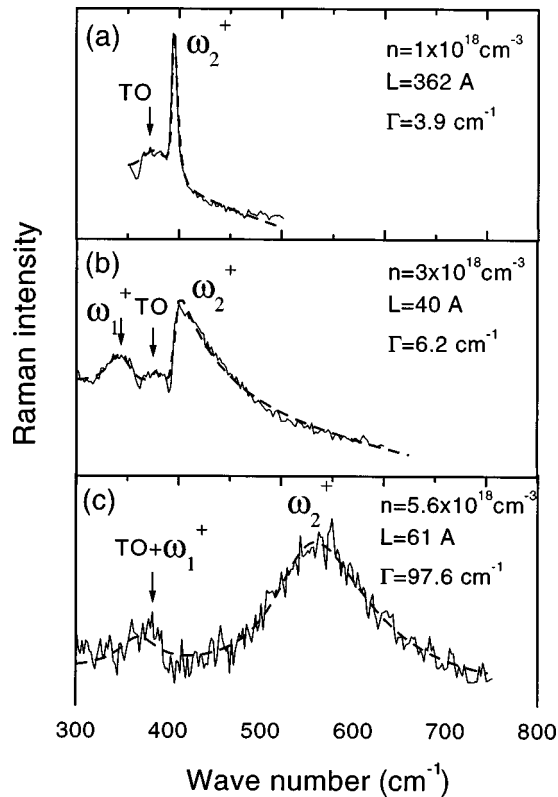


FIG. 4. The Raman spectra of doped $(\text{GaAs})_{17}(\text{AlAs})_2$ superlattices with different electron densities measured at $T=8$ K in the spectral range of AlAs-like optical phonons: $n=1 \times 10^{18} \text{ cm}^{-3}$ (a), $n=3 \times 10^{18} \text{ cm}^{-3}$ (b), and $n=5.6 \times 10^{18} \text{ cm}^{-3}$ (c).

$\times 10^{18} \text{ cm}^{-3}$ the calculated widths of the plasmon dispersions are 50, 112, and 175 cm^{-1} , respectively, while the corresponding half-widths of the plasmon-LO-phonon lines are 7.5, 52, and 130 cm^{-1} . Therefore, while in the lower

doped superlattice only a small part of the plasmon dispersion is involved, in the highly doped samples the situation is similar to that of the alloys—almost all the available plasmon states contribute to the Raman process. This shows the importance of the impurity potential fluctuations in doped superlattices.

It is worth mentioning that different localization lengths were observed in the superlattice where the Raman spectrum reveals well-defined GaAs and AlAs-like coupled modes (Fig. 3). We obtained $L \approx 89$ and 362 \AA for the GaAs-like (ω_1^+) and AlAs-like (ω_2^+) coupled modes, respectively. It is evident that the atomic vibrations contributing to the coupled modes are responsible for this difference. Therefore, in spite of the fact that the dispersions of the coupled modes are determined mostly by the plasmons, the phonon origin influences their localization lengths.

IV. CONCLUSIONS

The influence of a structural disorder on coupled plasmon-LO-phonon modes was studied in doped $\text{Al}_x\text{Ga}_{1-x}\text{As}$ alloys and in doped $(\text{GaAs})_n(\text{AlAs})_m$ superlattices. A relaxation of the momentum selection rules due to the breakdown in the crystal ordering was observed. This effect allows a large interval of the plasmon density of states to be involved in the Raman scattering. The analysis of the experimental results made it possible to determine the localization lengths of the carriers in the samples under investigation, and, thus, to estimate the range of the plasmon dispersion active in the Raman process; it further reveals the evidence of a metal-dielectric transition occurring in superlattices when the lowest miniband is completely filled.

ACKNOWLEDGMENTS

The financial support from CNPq, FAPESP, and CAPES is gratefully acknowledged.

¹H. Richter, Z. P. Wang, and L. Ley, *Solid State Commun.* **39**, 625 (1981).

²P. Parayanthal and F. H. Pollak, *Phys. Rev. Lett.* **52**, 1822 (1984).

³D. Olego and M. Cardona, *Phys. Rev. B* **24**, 7217 (1981).

⁴Yu. A. Pusep, S. W. da Silva, J. C. Galzerani, A. G. Milekhin, V. V. Preobrazhenskii, B. R. Semyagin, and I. I. Marahovka, *Phys. Rev. B* **52**, 2610 (1995).

⁵D. Pines, *Elementary Excitations in Solids* (Addison-Wesley, Reading, MA, 1963).

⁶Yu. A. Pusep, A. J. Chiquito, S. Mergulhão, and J. C. Galzerani, *Phys. Rev. B* **56**, 3892 (1997).

⁷T. Ando, A. B. Fowler, and F. Stern, *Rev. Mod. Phys.* **54**, 437 (1982).

⁸H. A. Fertig and S. Das Sarma, *Phys. Rev. B* **42**, 1448 (1990).